ARTICLE

OBC
www.rsc.org/obc

Photoaffinity labeling on magnetic microspheres (PALMm) methodology for topographic mapping: preparation of PALMm reagents and demonstration of biochemical relevance

Efrat Halbfinger,[a] Karine Gorochesky,[a] Sébastien A. Lévesque,[b] Adrien R. Beaudoin,[b] Larisa Sheihet,[c] Shlomo Margel[c] and Bilha Fischer*[a]

[a] *Department of Chemistry, Gonda-Goldschmied Medical Research Center, Bar-Ilan University, Ramat-Gan 52900, Israel*

[b] *Biology Sciences, University of Sherbrooke J1K 2R1, Canada*

[c] *Department of Chemistry, Bar-Ilan University, Ramat-Gan 52900, Israel*

Received 28th March 2003, Accepted 5th June 2003
First published as an Advance Article on the web 22nd July 2003

Photoaffinity labeling (PAL) is a technique widely used for identifying the binding-site within proteins. Although the classic method is both versatile and powerful, it suffers significant disadvantages, such as the need to radiolabel the PAL ligand, and the need to conduct highly complicated separations of both the labeled protein and the labeled peptides derived from it. Here, we propose a novel and universal methodology—Photo-Affinity Labeling on Magnetic microspheres (PALMm) designed to simplify and shorten the PAL protocol. In this context, we describe the preparation of PALMm reagents and the evaluation of their biochemical relevance regarding two ATP-binding enzymes: hexokinase and apyrase.

Introduction

The specific recognition between a protein and a bioactive ligand, occurs at a defined binding-site within the protein. The identification of a protein's binding-site, namely, the elucidation of the amino acid residues constituting the binding-pocket, is essential for understanding the protein function. Furthermore, this knowledge forms the basis for the design of new inhibitors/ligands for the regulation of enzyme/receptor activity.

A commonly used technique for identifying the binding/catalytic-site within proteins is topographic mapping.[1] Topographic labeling of a protein is defined as a labeling pattern that involves the full environment of a ligand within a binding-site. This method is suitable for proteins whose primary sequence is known. Topographic mapping is especially valuable when studying proteins for which X-ray crystal-structures are extremely difficult to obtain (*e.g.* membrane proteins). For topographic mapping, a photoaffinity labeling (PAL) protocol is usually applied.[1]

PAL protocol requires the use of a photoactiveable, but chemically inert, ligand analogue that is recognized by the protein's binding site.[1] For the detection of the ligand throughout the PAL protocol, the ligand is usually marked radioactively. Upon irradiation, the photreactive ligand, incorporated into the protein, transforms into a highly reactive species (nitrene or carbene) that inserts into neighboring covalent bonds. Identification of the resulting photo-crosslinked product provides structural information on the protein's binding site.

For this purpose, the photo-crosslinked protein is separated from the free protein and then subjected to enzymatic degradation. Subsequently, the resulting labeled protein fragments are separated from the multitude of peptides. Finally, the labeled peptides are analyzed by Edman degradation or mass spectroscopic methods to identify labeled amino acids that constitute the protein's binding-site.

To obtain as complete mapping as possible, the PAL reagent is required to have a dynamic interaction, allowing the probe to adopt different positions in the binding site. Furthermore, photoprobes with the highest possible photoreactivity, are required to enable reaction with a maximum number of amino acids in the binding site. The photoreactive group should be chemically stable, with the longest possible wavelength of irradiation in order to avoid damage to the protein (>280 nm). Azides, diazirines, and diazonium salts used for photoaffinity labeling are usually fluoroaromatic derivatives in order to increase their chemical stability.[1b–3] Although highly reactive species are formed, non-specific labeling is usually limited, due to efficient quenching of the photogenerated species by the solvent.[1a]

The versatile and powerful PAL method has been applied in numerous structural studies. For instance, the PAL method provided a detailed picture of ion channels,[4] transporter proteins,[5] and nucleic acid–protein interactions.[1e] Photoaffinity labeling was used to probe RNA–RNA contacts,[6] and protein–protein interactions, for studying signal transduction.[7] The PAL method was also harnessed for drug discovery and development.[1d,f]

A critical step in the PAL method is the synthesis of the PAL ligand. The additional synthetic steps, required for the introduction of photosensitive groups and radiolabels to the ligand, complicate this technique. Furthermore, the PAL protocol involves two highly complicated separations: separation of the photo-crosslinked protein from the hardly distinguishable free protein; and, separation of the peptides marked by the photoaffinity label from the multitude of non-labeled peptides. HPLC separation of the tryptic digest results in a crowded chromatogram with overlapping peaks.[8,9] The identification of the HPLC peaks containing the labeled peptides is yet another complication.[8a,b]

Thus, the commonly used photoaffinity labeling remains a labor-intensive method from the synthesis of the PAL reagent to sequencing the labeled peptides.

Several improved PAL methodologies have been reported. For instance, the replacement of a radioactive marker by a fluorescent one made the classic PAL method easier to implement. Fluorescent marking is achieved by either binding the ligand to a photoactiveable, fluorescent reagent,[10] or by extending the ligand bearing a photoactiveable part to form a fluorescent molecule.[11] Nevertheless, the use of a fluorescent marker still did not solve the problem of complicated purifications, required in the PAL protocol. However, conjugating the ligand

DOI: 10.1039/b303425a

to a biotin marker helped to avoid radioactive labeling, and to simplify the purification steps.[9,12] Yet, this method does not completely exclude the use of HPLC.[9] Furthermore, this method requires an additional step of chemiluminescent detection of the labeled peptides,[9] or alternatively, the addition of a fluorescent marker.[12b] Thus, the limitations of the various PAL methods justify the continued search for improved topographic mapping techniques.

Here, we propose a novel and universal PAL methodology—Photoaffinity Labeling on Magnetic microspheres, denoted as PALMm. This method is designed to overcome the above-mentioned limitations of the PAL technique. We describe the preparation of PALMm reagents **1** and **2** and the evaluation of their biochemical relevance regarding two ATP-binding enzymes: hexokinase and apyrase. The application of the novel PALMm reagents **1** and **2** for the topographic mapping of these enzymes will be reported in due course.

Results and discussion

Description of the PALMm methodology

The PALMm protocol, outlined in Fig. 1, is based on the classic PAL method, yet, it presents several significant improvements. These improvements are made possible by the use of PALMm reagents (*e.g.* **1** and **2**). Specifically, this PALMm method includes the following steps. 1. Incubation of the protein with a photoactiveable PALMm ligand bound to magnetic microspheres. 2. Irradiation of the ligand–protein complex at a specific wavelength that produces a highly reactive ligand species (*e.g.* carbene), which inserts into a covalent bond of a near-by amino acid residue. 3. Magnetic separation of the photo-cross-linked protein from the free protein. 4. Enzymatic digestion of the labeled protein. 5. Magnetic separation of microsphere-linked peptides from the tryptic digest. 6. Detachment of peptides from the magnetic microspheres by reduction of a disulfide bond. 7. Identification of labeled amino acid residues that constitute the protein's binding-site by ESI MS/MS analysis of the peptides. 8. Correlation of mass spectroscopic results with biochemical and site-directed-mutagenesis data for the final topographic mapping.

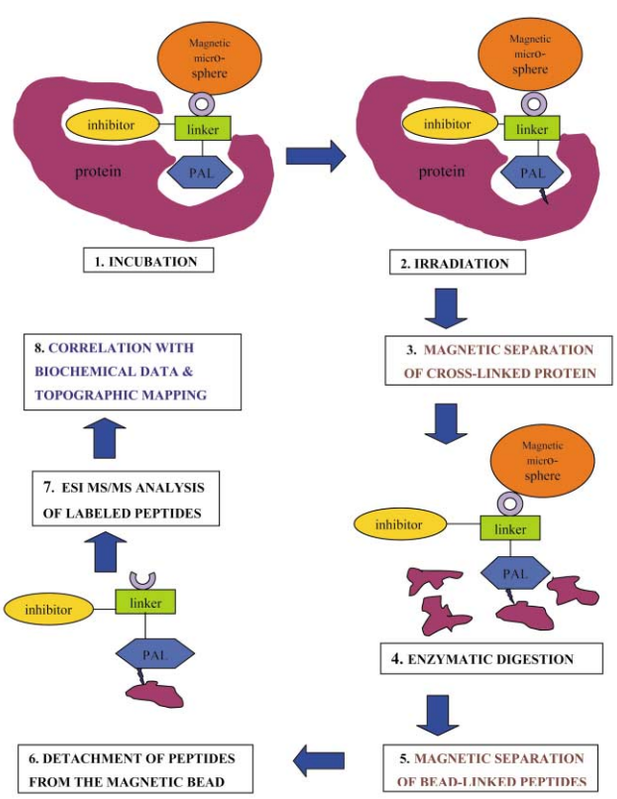

Fig. 1 A proposed protocol for topographic mapping by Photo-Affinity Labeling on Magnetic microspheres—PALMm.

The proposed PALMm methodology is expected to shorten considerably the labor and time required to perform PAL studies. One of the primary expected advantages of the PALMm methodology is the cessation of the need to conduct radiolabeling of the PAL reagent. In addition, the PALMm methodology is expected to extremely simplify isolation steps (steps 3, 5, Fig. 1). Separation of the cross-linked protein from the free protein is made possible by 'fishing' it out magnetically. Furthermore, the proposed methodology prevents the need of complicated separations on HPLC of the multicomponent mixture of peptides obtained after enzymatic degradation of the crosslinked protein. In our methodology, HPLC separation would not be required due to the limited number of labeled-peptides expected to be 'fished' out magnetically (steps 5, 6), and the further use of the ESI MS/MS technique (step 7).

Selection of a scaffold for PALMm reagents

The above-mentioned PALMm methodology is expected to serve as a universal means for topographic mapping. Here, we describe the compatibility of PALMm reagents **1** and **2** for the topographic mapping of several ATP-binding proteins. Specifically, we focused on hexokinase, whose binding-site is well characterized,[13–17] and on apyrase whose catalytic-site has not yet been deciphered. Hexokinase is targeted as a model for proving the feasibility of the PALMm method. Once the known ATP-binding-site of hexokinase is reproduced by the PALMm method, we can then apply this method for elucidating the unknown catalytic-site of apyrase.

As shown below, the elucidation of this catalytic-site is a prerequisite for the design of novel drugs regulating nucleotide signaling. Specifically, the major effects of ATP-receptors (including P2Y-R and P2X-R subtypes)[18,20] on most of the physiological systems[18b,21–25] are modulated by metabolic enzymes.[26] Among the key enzymes involved in the regulation of extracellular nucleotide concentrations in the vicinity of ATP-receptors, apyrases (NTPDases) play a major role in hydrolyzing tri- and/or di-phosphate-nucleosides to monophosphate-nucleosides.[27]

The first member of this family, NTPDase1, was found, purified, and characterized by Lebel *et al.*[28] Its kinetic properties, substrate specificity, and influence of certain inhibitors were later described.[29,30] Sequence analysis and directed mutagenesis on apyrase conserved regions (ACR) have indicated that two ACRs (I and IV) play an essential role in catalytic activity of NTPDases.[31,32] Yet, substrate specificity may also depend on other regions of the protein because the NTPDases which share the ACR, exhibit different rates of catalysis with tri- and di-nucleosides. In this respect, one cannot exclude that sequences in the vicinity of these conserved regions have a role to play in substrate specificity.[33] Therefore, it is essential to define the topographic configuration of the active-site. This step is a prerequisite in the design of potent and specific inhibitors of these key enzymes that regulate nucleotide signaling.[34]

For the topographic mapping of NTPDase (apyrase) we designed suitable PALMm reagents based on our previously developed inhibitors of NTPDase.[35]

Earlier, we identified 8-substituted ATP derivatives **3a**–**c** (Scheme 2) as very poor P2Y-R ligands. Therefore, these analogues served as an attractive scaffold for the development of specific NTPDase inhibitors.[36] On the basis of the promising hydrolytic stability of derivatives **3a**–**c** regarding NTPDase,[35] a new series of 8-thioether ATP analogues, **3d**–**g**, was explored.[35] Among these analogues, 8-BuS-ATP was found as a competitive inhibitor with the lowest K_i value, 10 μM; where 8-CH_2-tBuS-ATP, 8-cycloheptylS-ATP and 8-hexylS-ATP analogues produced a mixed type of inhibition. 8-BuS-ATP, **3a**, was found

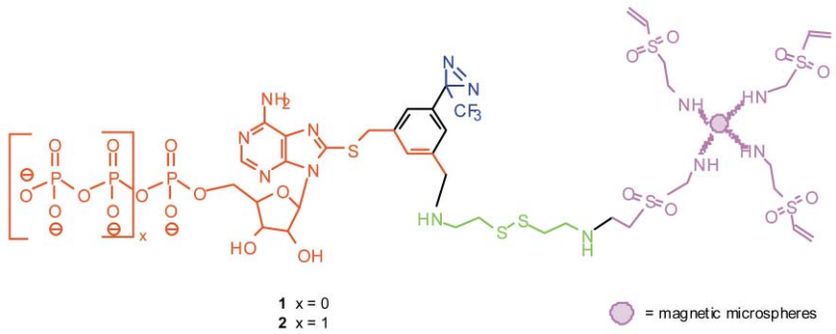

Scheme 1 Structures of nucleotide-based PALMm reagents.

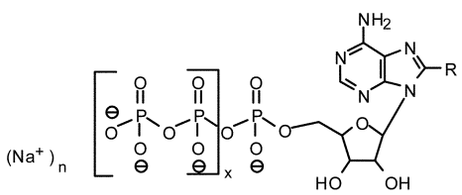

3a R = $S(CH_2)_3CH_3$ x = 1

3b R = $NH(CH_2)_3CH_3$ x = 1

3c R = $O(CH_2)_3CH_3$ x = 1

3d R = SC_7H_{13} x = 1

3e R = $SCCH_2(CH_3)_3$ x = 1

3f R = SCH_2CH_3 x = 1

3g R = $S(CH_2)_5CH_3$ x = 1

3h R = $S(CH_2)_3CH_3$ x = 0

Scheme 2 Structures of NTPDase inhibitors.

both to be the most effective non-hydrolyzable competitive inhibitor, and also a specific inhibitor having no interaction with P2X-receptors,[35] and $P2Y_1$-receptors.[36]

Based on these findings, we selected derivative **3a** as an attractive scaffold for the preparation of PALMm analogues **1** and **2**, targeting NTPDase and possibly other ATP-binding proteins.

Design of PALMm reagents

To implement the PALMm protocol, we propose special reagents, *e.g.* **1** and **2** (Scheme 1). These reagents are composed of five moieties (Scheme 3): A) inhibitor precursor (**4**); B) a compact tri-functional aromatic linker (in **5**); C) a small PAL moiety (diazirine) (in **5**); D) a magnetic bead (**6**); E) a cleavable spacer between the aromatic linker and the magnetic bead (**7**).

A Inhibitor. A specific inhibitor is required for targeting the PAL moiety to the enzyme's catalytic-site. This inhibitor should have affinity towards the target protein, yet not high affinity, in order to enable maximal labeling of the binding-site. Since we aim to map the unknown catalytic-site of apyrase, we chose an apyrase (NTPDase) inhibitor, **3a**, which we previously developed,[35] as a scaffold for the construction of the related PALMm reagents **1** and **2**. PALMm reagent **1** was first evaluated as both a substrate and inhibitor of hexokinase. This enzyme serves here as a structurally known model for proving the feasibility of the PALMm method.

B Photoaffinity label. The photoaffinity label of choice should be chemically stable during the preparation of the PALMm reagent. Furthermore, the wavelength of irradiation of the PAL moiety should be as long as possible, far from that absorbed by proteins, in order to avoid damage to the enzyme. The photoaffinity label of choice was 3-(trifluoromethyl)-3-phenyldiazirine[3a,37] (in **5**), which is chemically stable in mild acidic or basic environments,[38] and is irradiated at a non-destructive wavelength (*ca.* 360 nm).

C linker. The diazirine PAL moiety has to be linked to the inhibitor scaffold, **4**, and to the magnetic bead, **6**, through a chemically and enzymatically stable bond. Thus, the linking groups of choice are amine and thioether, which are stable under the synthesis conditions and the PALMm protocol conditions (Fig. 1). The linker between the diazirine and inhibitor precursor **4**, should be as short as possible to enable maximum proximity of the PAL moiety to the inhibitor, and therefore ensure labeling of the catalytic-site. The linker of choice is *m*-xylyl (in **5**), where the distance between the inhibitor precursor **4** and the diazirine PAL moiety is only four atoms long (*e.g.* in product **13**, Scheme 5).

D Cleavable spacer. A cleavable spacer, **7**, is required to enable the detachment of the inhibitor-linked-peptide from the

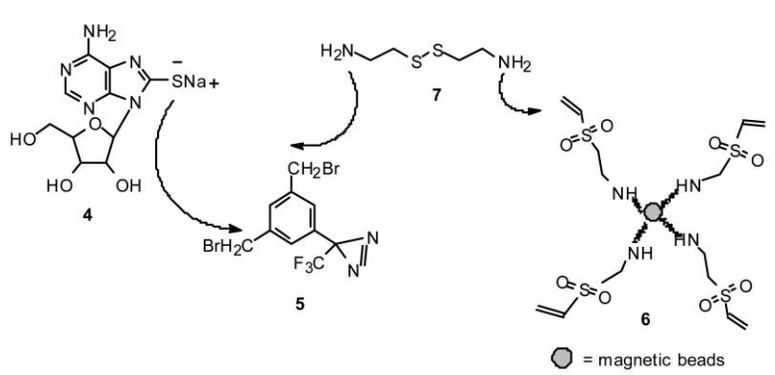

Scheme 3 General scheme for the preparation of a PALMm reagent.

functionalized magnetic microsphere (step 6, Fig. 1). This cleavage should be performed under mild conditions that would not harm any functions of the inhibitor or the bound peptide. For this purpose, cystamine is used as a cleavable spacer. Cystamine is attached *via* one amino end to the linker, **5**, and *via* a second amino end to the magnetic microsphere, **6** (Scheme 3). The peptide-bound inhibitor can be detached from the bead by dithiotriethol or tris(2-carboxyethyl)phosphine[39] reduction of the cystamine's disulfide bond.

E Magnetic microsphere. The proposed magnetic microspheres, **6**, consist of polystyrene microspheres of a narrow size distribution, *ca.* 6 micron diameter. These particles are coated with magnetite (Fe_3O_4), and then with silica[40a] bearing vinyl sulfone functions.[40b–d]

Assembly of PALMm reagents 1 and 2

PAL reagent **5**, is attached *via* one methylene bromide group, to a precursor of apyrase inhibitor, **4**, and *via* the other methylene bromide, to a cystamine cleavable spacer, **7** (Scheme 3). The resulting nucleoside is then phosphorylated at the 5′ position of the sugar, and finally the cystamine moiety, is added through its free amine, to the vinyl sulfone derivatized magnetic bead, **6**. The detailed assembly of PALMm reagents is described in Schemes 4–6.

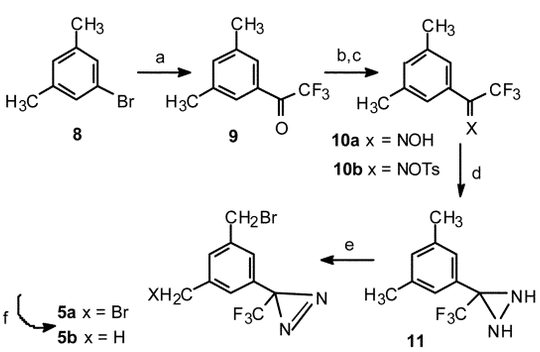

Scheme 4 Synthesis of PAL moiety bearing suitable linkers. *Conditions*: a. 1. BuLi, 2. CF_3CO_2Me, 92%; b. $HONH_2$, 97%; c. TsCl; d. NH_3 (g); e. 3 eq NBS, $(PhCOO)_2$, 25% (**5a**); 51% (**5b**); f. 1 eq NBS, 64% (**5a**).

5-Bromo-1,3-xylene, **8**, served as a scaffold for the PAL moiety generation (Scheme 4). The brominated position was elaborated by BuLi and methyl trifluoroacetate to form a ketone **9**. Three equivalents of BuLi were required to obtain product **9** in 92% yield. Ketone **9** was converted to diaziridine **11** in three steps in 97% overall yield.[41] Next, each of the benzylic positions was mono-brominated by NBS in methyl formate in the presence of dibenzoyl peroxide under light (either sunlight or fluorescent lamp).[42] Under these conditions, the diaziridine function in **11** was also oxidized to the corresponding diazirine to form the desired PAL reagent, **5a**. This was indicated by instant-

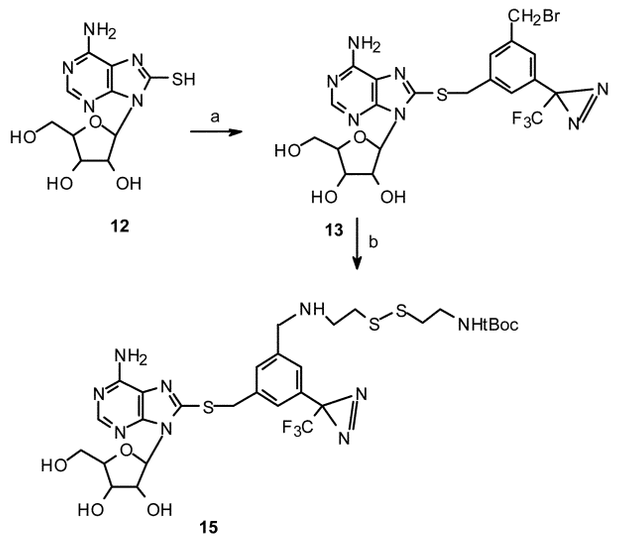

Scheme 5 *Conditions*: a. 1. NaOH, 2. **5a**, 4 h, 57%; b. $H_2N(CH_2)_2$-$SS(CH_2)_2NHtBoc$, **14**, 42%.

aneous loss of the purple ninhydrin-colored spot of **11** from the TLC plate, and the appearance of a typical diazirine absorption at 360 nm. NBS, was found to be a mild diaziridine oxidizing agent, as compared to other reagents used for this purpose such as: $AgNO_3$, Ag_2O, I_2, CrO_3, $NaIO_4$, and RuO_2.[43] This diazirdine oxidation occurs probably *via* a radical mechanism leading to the formation of HBr and succinimide, in addition to diazirine. Optimized conditions of the reaction, avoiding the formation of multi-brominated products, involved the addition of three equivalents of NBS. Under these conditions, the desired PAL reagent **5a** was obtained in 25% yield. This product was accompanied with the mono-brominated product, **5b**, obtained in 51% yield, which was then recycled with 1 eq NBS to form **5a** in 64% yield.

PAL reagent **5a** was linked to a precursor of apyrase inhibitor, **4**, *via* a thioether bond (Scheme 5). Selective S-monoalkylation of nucleoside **12** by **5a** was achieved by first preparing the sodium thiolate salt **4**,[35] and then adding it to a highly dilute solution of **5a** at room temperature. The resulting nucleoside, **13**, obtained in 57% yield, was then coupled to the cleavable spacer cystamine. To avoid the di-alkylation of cystamine by **13** and the phosphorylation of the cystamine's free amine in the next synthetic step (Scheme 6), cystamine **7**, was mono-protected by t-Boc group.[44] This group is stable under conditions of the alkylation step forming **15** and the phosphorylation steps leading to **16** and **17** (Scheme 6). Nucleoside **13** was, therefore, treated with 5 eq mono-protected tBoc-cystamine, **14**, in the presence of a basic resin (Dowex MWA-1) in DMF to provide product **15** in 42% yield. The last synthetic step before coupling the reagent to the magnetic microspheres, included the preparation of nucleotides **16** and **17** by phosphorylation of the 5′-position of nucleoside **15**. Under the conditions of one-pot 5′-triphosphorylation, involving the addition of $POCl_3$ in

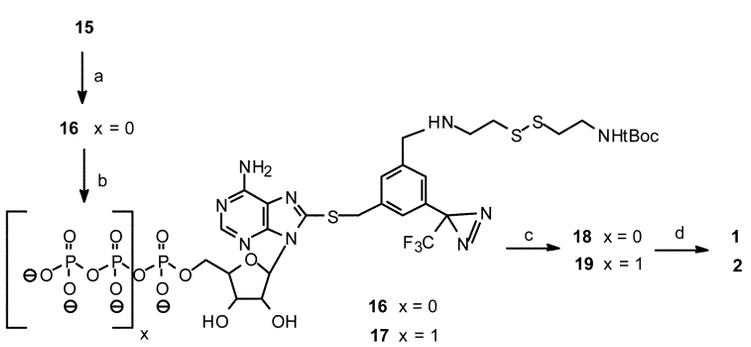

Scheme 6 *Conditions*: a. 1. $POCl_3$, $PO(OMe)_3$, 31%; b. 1. 10 eq CDI, 2. $P_2O_7(Bu_3NH^+)_4$, 20%; c. TFA, quantitative yield; d. pH 8.6, **6**, high dilution.

$PO(OMe)_3$ at 0 °C followed by bis(tributylammonium)-pyrophosphate and then hydrolysis,[45] only the 5′-monophosphate product **16** was obtained in low yield. All attempts to modify the phosphorylation conditions for obtaining nucleoside 5′-triphosphate **17** failed.

Since our goal was the preparation of PALMm reagents targeting ATP-binding proteins we attempted the preparation of **17** by a convergent synthesis starting from a precursor **20**, bearing already the triphosphate moiety at 5′-position to which compound **22**, that includes the linker, PAL, and spacer moieties, will be attached (Scheme 7).

8-SNa-ATP, **21b**, was prepared in 48% yield from 8-Br-ATP, **20**, in a 2 M NaSH solution, pH 8,[46] followed by treatment of **21a** with NaOH, pH 11. The product was identified by spraying the TLC plate with Ellman's reagent, dithiobis(nitrobenzoic acid), and sodium sulfite,[47] thus forming an indicative yellow spot. For the preparation of compound **22**, PAL reagent **5a** was treated with monoprotected tBoc-cystamine, **14**, in the presence of DOWEX-MWA-1 (basic resin). This reaction required an excess of **5a** and high dilution to avoid the reaction of tBoc-cystamine with both benzylic positions of **5a**. However, product **22** was obtained in a minute amount accompanied by a complex mixture of products.

Eventually, the preparation of pre-PALMm reagent **17** was achieved in two steps (Scheme 6). The first step included monophosphorylation of nucleoside **15** with $POCl_3$ in $PO(OMe)_3$ to obtain **16** in 31% yield. The second step included di-phosphorylation of nucleoside-5′-monophosphate **16**, to produce the triphosphate homologue **17**, using an activating agent 1,1′-carbonylbis(imidazole) (CDI), and bis(tetrabutylammonium)-pyrophosphate.[48] The 5′-phosphorimidazolidate intermediate, formed from **16** and CDI, facilitates the nucleophilic attack of the pyrophosphate salt.[48] The desired nucleotide **17**, obtained in 20% yield, was characterized by ^1H and ^{31}P NMR, UV, and FAB spectra.

Next, the t-Boc protecting group was carefully removed in neat TFA, for 3 min, to produce the desired product **19** in a quantitative yield. With constant nitrogen gas flow and a short reaction time, the decomposition of the triphosphate chain was almost completely prevented. In the same way, the t-Boc protecting group was removed from the homologue **16** to provide nucleotide **18**.

Pre-PALMm reagents **18** and **19**, with free amine side-chain, were coupled to the magnetic microspheres **6** *via* a Michael addition to vinyl sulfone groups on the bead at pH 8.6. As described below, this was performed under high dilution, to provide the desired PALMm reagents **1** and **2**.

Characterization of magnetic microspheres 6

Magnetic microspheres, **6**, consisting of polystyrene microspheres (*ca.* 6 micron diameter), coated with Fe_3O_4 and then with amine group bearing silica,[40a] were functionalized with divinyl sulfone (DVS). This provided active olefin functions for coupling with amines **18** and **19**.[40b–d] The number of vinyl sulfone functions (free binding sites) on the magnetic microspheres was quantified as follows.

An excess of mercaptoethanol in $NaHCO_3$ solution (pH 8.6) was added to magnetic microspheres, **6**. After overnight reaction, that produced **23** (Scheme 8A), the microspheres were removed with a magnet and washed. The filtrate was analyzed for its mercaptoethanol content with an excess of 4,4′-dipyridyl disulfide, 4-PDS, **24** (Scheme 8B). 4-PDS reacts with thiols and produces 4-thiopyridone, 4-TP, **25**.[49] Product **25** has a typical absorption at 323 nm, far enough from that of **24** (247 nm), thus minimizing the overlap of the UV bands of starting material and product. This minimal overlap enabled the determination of mercaptoethanol concentration in the filtrate based on 4-TP's absorbance and ε (13 251 cm^{-1} M^{-1} at 323 nm in 0.1 M sodium bicarbonate buffer, pH 8.6). The number of moles of reacted mercaptoethanol provided the number of free binding-sites on microspheres **6** (7.7 μeq per 1 mg microspheres).

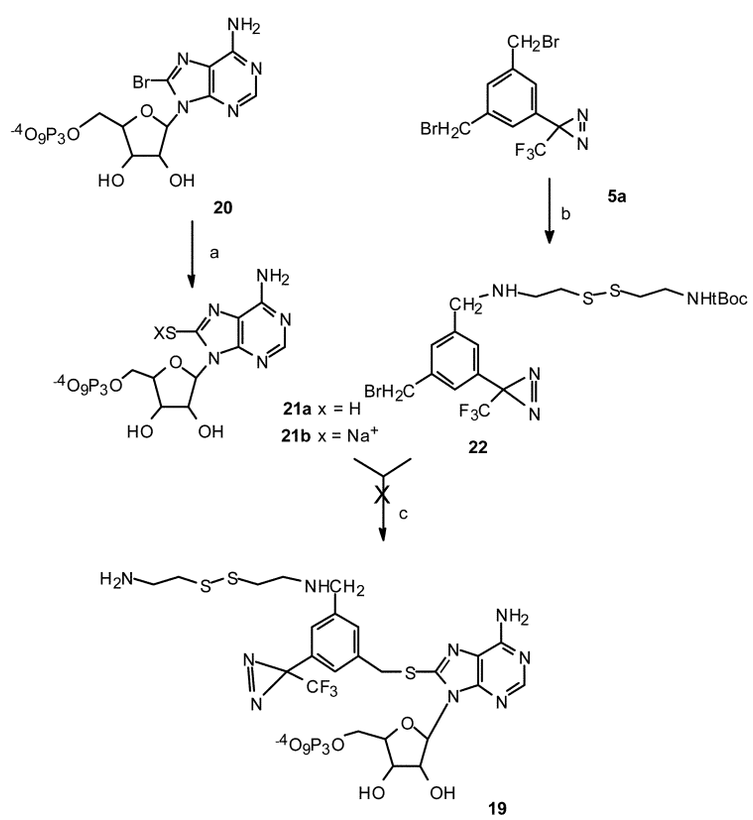

Scheme 7 *Conditions*: a. 1. NaSH, RT, overnight, 2. NaOH, pH 11, 48%; b. $H_2N(CH_2)_2SS(CH_2)_2NHtBoc$, **14**, 80 °C 3 h, 2 eq DOWEX-MWA-1, acetonitrile; c. 1. DOWEX-MWA-1, DMF, 2. TFA, 3 min.

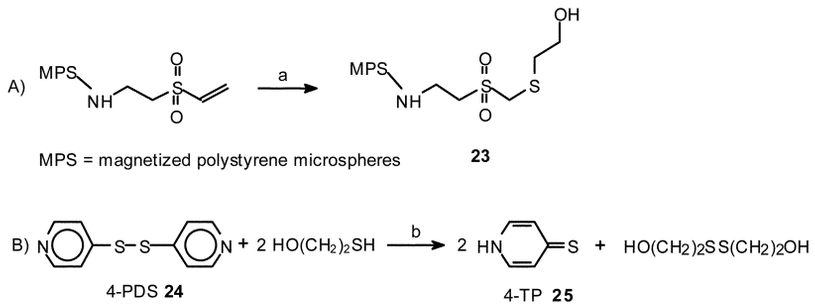

Scheme 8 *Conditions*: a. $HO(CH_2)_2SH$, RT, overnight, 0.1 M $NaHCO_3$ pH 8.6; b. 0.1 M $NaHCO_3$ pH 8.6, 5 min.

Table 1 Percentage of phosphoryl group transfer by hexokinase in the presence of ATP and/or nucleotide analogues

Nucleotide analogue	Relative % of hexokinase activity
ATP	100 [a]
8-BuS-ATP, **3a**	58 [a]
PALMm reagent **2**	23 [a]
8-BuS-ATP, **3a** + ATP	76 [b]
8-BuS-AMP, **3h** + ATP	100 [b]
PALMm reagent **2** + ATP	100 [b]

[a] Evaluation of 8-BuS-ATP as a co-substrate compared to ATP. Assays were performed for 5 min at 25 °C with 0.025 units protein and 8-BuS-ATP, **3a**, or ATP (370 μM of each) in the incubation medium. Reagent **2** was assayed at 890 μM concentration. Assays were performed in duplicate (SEM 0.013). [b] Evaluation of 8-BuS-ATP, **3a**, and 8-BuS-AMP, **3h**, as inhibitors of phosphoryl group transfer from ATP. Assays were performed for 5 min at 25 °C with 0.025 units protein, 8-BuS-ATP or 8-BuS-AMP and ATP (370 μM of each). Assays were performed in duplicate (**3a**, SEM 0.0085) or triplicate (**3h**, SEM 0.039). Reagent **2** was assayed at 500 μM concentration.

Coupling PALMm reagents 18 and 19 to magnetic microspheres 6

Pre-PALMm reagents **18** and **19** were then coupled overnight to magnetic microspheres **6** in bicarbonate buffer, pH 8.3. The products, PALMm reagents **1** and **2** (Scheme 1), were subsequently separated from the solution by a strong magnet. The yield of the coupling reaction in both cases was *ca.* 70% based on the amounts of **18** and **19** remaining in the solution, as determined through their absorbance at 285 nm (ε 20955 M^{-1} cm^{-1}).

Evaluation of PALMm reagent 2 as a substrate/inhibitor of hexokinase

The compatibility of reagent **2** for a PALMm protocol was evaluated by first studying its affinity to the primary target enzyme, hexokinase. The reproduction of the known binding-site of hexokinase [13–17] by the PALMm protocol, with reagent **2**, will validate this method and will enable its application for structurally unknown proteins (*e.g.* NTPDase/apyrase) as final targets.

PALMm reagents **1** and **2** were designed and synthesized based on the inhibitor of the final target, NTPDase, namely, based on 8-BuS-ATP **3a**.[35] Therefore, for proving the affinity of reagent **2** to hexokinase, we initially had to determine the ability of the model compound, 8-BuS-ATP, **3a**, to bind to hexokinase, as either a co-substrate or an inhibitor.

8-BuS-ATP, **3a**, was first evaluated as a co-substrate for hexokinase,[50] and the percentage of phosphoryl group transfer to glucose was compared to that of ATP (Table 1). Next, 8-BuS-ATP and 8-BuS-AMP were evaluated as inhibitors of hexokinase, at a concentration of 370 μM for each (Table 1). 8-BuS-ATP was found to be a moderate substrate for hexokinase, producing about 58% activity compared to that of ATP. The inhibitory effect of **3a** was modest, reducing hexokinase activity to about 76%. 8-BuS-AMP, **3h**, however, did not inhibit the reaction of ATP at all.

Once the affinity of the model compound **3a** to hexokinase had been demonstrated, we set to evaluate PALMm reagent **2**, as either a co-substrate or inhibitor of hexokinase. First, the bead-bound nucleotide **2** at 890 μM concentration, was suspended in the solution containing the assay's enzymes (hexokinase and glucose-6-phosphate dehydrogenase) and reagent (β-NADP),[50] and the enzymatic reaction was monitored by UV for 20 min (Fig. 2). During the first five minutes of the assay, in addition to the absorbance of β-NADPH, the absorbance of magnetic microspheres, **6**, which are scattered in the solution, is also observed (Fig. 2). The elevation of the spectrum's baseline is due to the black opaque color of the particles (Fig. 3). The

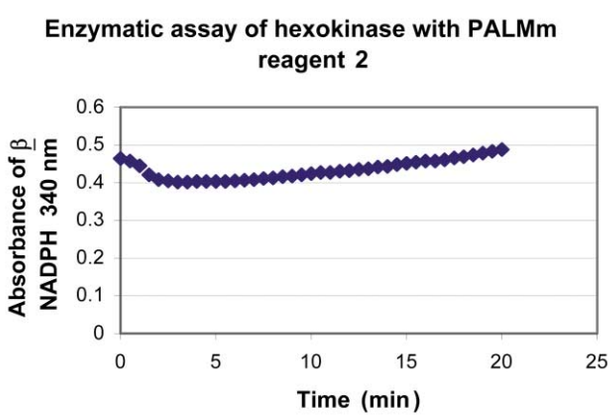

Fig. 2 Evaluation of PALMm reagent **2** as a hexokinase co-substrate. The reaction of hexokinase is monitored by the change of β-NADPH absorbance at 340 nm. The elevated absorbance during the first minutes is due to the scattered magnetic microspheres (Fig. 3). After 5 min, microspheres **2** sank down and a linear increase of β-NADPH absorbance was measured. For calculating the enzyme activity we used absorbance data from the 5th min onwards.

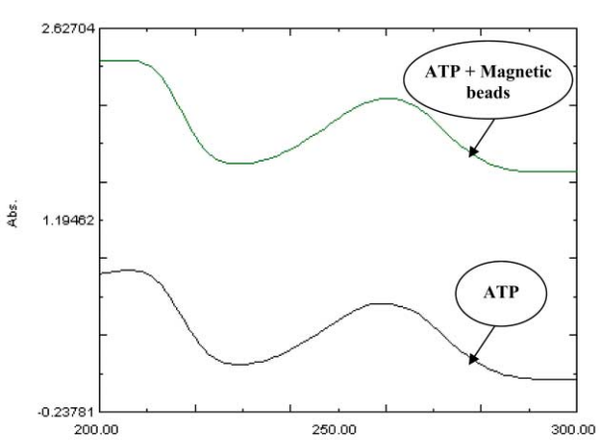

Fig. 3 Magnetic microspheres **6** elevate the baseline of the UV spectrum. A) ATP solution. B) ATP solution and 1 mg of microspheres **6**.

absorbance of β-NADPH alone is measured *ca.* five minutes after the beginning of the assay, when the suspended magnetic microspheres sink. Calculation of percentage of phosphoryl group transfer uses absorbance data from the fifth minute onwards.

PALMm reagent **2** was found to be a weak co-substrate of hexokinase with only 23% phosphoryl-group transfer, as compared to ATP at the same concentration. PALMm reagent **2** was then evaluated as a potential hexokinase inhibitor, in the presence of an equimolar amount of ATP (500 μM), and the enzyme's activity was compared to that with ATP alone. PALMm reagent **2** had practically no inhibitory effect.

Evaluation of PALMm reagent 1 as an inhibitor of apyrase

After demonstrating the affinity of PALMm reagent **2** to the primary target enzyme, hexokinase, we aimed to evaluate the affinity of reagents **1** and **2** towards the final target: apyrase.

This goal was achieved in three sequential and dependent steps. First, a model compound, 8-BuS-AMP, **3h**, was tested as an inhibitor of NTPDase1, with ATP as the substrate. In the second step, pre-PALMm reagent **16**, which is water-soluble and still not bead-bound, was used as a model compound for PALMm reagent **1** and was evaluated as an NTPDase1 inhibitor. In the third step, after demonstrating the affinity of **16** to NTPDase, the corresponding bead-bound reagent **1** was evaluated as a potato-apyrase inhibitor. Potato-apyrase was chosen as a model to characterize the NTPDase(s) active site, since it contains all five conserved regions (ACR I to V), possesses similar activity to NTPDase1, and has 20.3% to 28.7% identity to known mammal NTPDases. Yet, practically, potato-apyrase is much easier to study because, unlike NTPDase1, it is water-soluble and stable (loss of less than 10% activity after two weeks at 4 °C).[51]

The activity of the enzyme was measured based on the strong absorbance at 630 nm of the complex of malachite green with Pi released upon hydrolysis of ATP by NTPDase1 or apyrase.[52,53]

Thus, in the first step it was found that the activity of the enzyme decreased to 18% at 100 μM concentration of 8-BuS-AMP (Fig. 4A). This significant inhibition prompted us to explore the inhibitory potential of pre-PALMm reagent **16** as a soluble model of PALMm reagent **1**. Pre-PALMm reagent **16** at 100 μM indeed decreased the activity of NTPDase, yet, only to 68% of that of ATP (Fig. 4B).

Next, the bead bound reagent **1**, at 1260 μM concentration, was evaluated as a potato-apyrase inhibitor with an equimolar concentration of ATP as the substrate. PALMm reagent **1** was found to be a poor inhibitor of apyrase that decreases the hydrolysis rate of ATP to 83%. Namely, reagent **1** demonstrates a weak interaction with apyrase.

Summary

The essence of the PALMm method, proposed here to overcome the severe limitations of the classic PAL protocol, is the utilization of a PALMm reagent (*e.g.* **1** or **2**), which is a trifunctional affinity probe bound to a magnetic microsphere. Specifically, we prepared here PALMm reagents targeting adenine-nucleotide binding proteins.

Several adenine nucleotides bearing a PAL moiety have been previously prepared for incorporation in DNA, yet they bear the PAL moiety on the adenine's N^6-amine,[54] the phosphate backbone,[55] or on the ribose.[1e]

Here, we considered that keeping free N^6-position, phosphate, and ribose moieties, is essential for the molecular recognition of the ATP-analogue by the protein. Therefore, we attached the functionalized PAL moiety at the C8-position of the nucleotide. Furthermore, we based this decision on the pronounced inhibitory effects of 8-BuS-AMP and 8-BuS-ATP, shown in this and previous studies.[35]

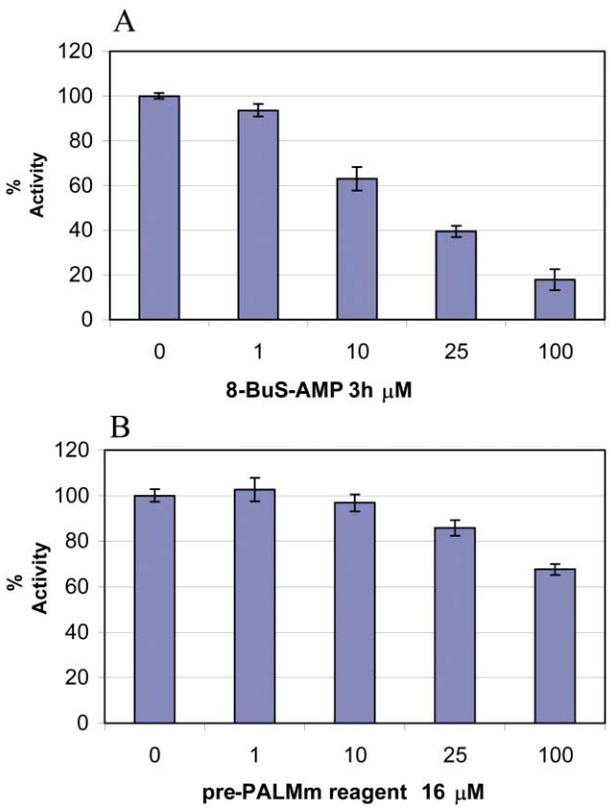

Fig. 4 Influence of 8-BuS-AMP and pre-PALMm reagent **16** on NTPDase1 ATPase activity. Assays were performed for 7 min at 37 °C in the presence of 1.0 μg of protein and different concentrations (1 to 100 μM) of 8-BuS-AMP and pre-PALMm reagent **16** in the incubation medium. Reactions were started by adding 100 μM of ATP. A) A concentration dependent inhibition of NTPDase1 ATPase activity is observed for 8-BuS-AMP up to (82.2 ± 4.7%) at 100 μM. B) For compound **16** there is a weak inhibition (32.4 ± 2.4% at 100 μM). Results are the mean of triplicate samples. The maximum deviation from the mean was within 10%.

The construction of the PALMm reagent on the scaffold of 8-BuS-ATP raised the following questions. Will the binding-site of apyrase/hexokinase accommodate ATP analogues bearing a large substituent at C8 (*e.g.* analogues **16**–**19**)? Will the magnetic microsphere **6**, which is *ca.* 100-fold larger than the protein, interfere with nucleotide binding to the protein?

For assessing the biological relevance of PALMm reagents **1** and **2**, we evaluated them as either substrates or inhibitors of hexokinase and apyrase.

PALMm reagent **2** was identified as a weak hexokinase substrate demonstrating 23% phosphoryl group transfer compared to that of ATP. Likewise, PALMm reagent **1** was identified as a weak inhibitor of potato-apyrase, reducing the percentage of hydrolysis of ATP to 83%. The affinity of these reagents to the corresponding enzymes is low compared to their precursors. For instance, 8-BuS-ATP is a moderate substrate of hexokinase with 58% enzyme activity compared to ATP, while reagent **2** is a weak substrate (23%). Likewise, 8-BuS-AMP is an NTPDase1 inhibitor reducing the activity of the enzyme to 18% compared to ATP; while pre-PALMm reagent **16**, a soluble model of reagent **1**, and reagent **1** decreased the activity only to 68% and 83%, respectively.

The reduction in substrate/inhibitor nature of the PALMm reagents compared to their precursors may be due to either the bulkiness of the substitution at C8, or hindrance of the magnetic particle. However, such hindrance is less likely because the 17-atoms long flexible spacer between the inhibitor and the microsphere (from the aromatic ring on the inhibitor to the silica surface of the microsphere) is expected to enable free approach of the protein to the particle-bound-inhibitor.

It is known that the reagents used for PAL studies should not bind to the protein too strongly. This is necessary in order to enable their binding to as many amino acid residues as possible to obtain as complete as possible structural information on the binding-site.[1] Therefore, PALMm reagents **1** and **2**, found to be a weak inhibitor and substrate, respectively, are suitable for the PALMm protocol.

The PALMm approach is universal and may be in principle applied to the topographic mapping of any protein, provided the PALMm reagent is based on the appropriate inhibitor/ligand scaffold. Here, we demonstrated the biochemical relevance of 8-substituted-adenosine-nucleotide PALMm reagents **1** and **2** regarding two ATP-binding proteins—hexokinase and apyrase. The application of reagents **1** and **2** for the topographic mapping of these enzymes will be published in due course.

Experimental

General

^{1}H spectra were measured at 200, 300, or 600 MHz on Bruker AC-200, DPX-300, or DMX-600 spectrometers. ^{13}C NMR spectra were measured at 75.4 MHz on Bruker AC-200, DPX-300, or DMX-600 spectrometers. The chemical shifts are reported in ppm relative to tetramethylsilane (TMS) as an internal standard. ^{19}F NMR spectra were measured on Bruker AC-200, using $CFCl_3$ as an external reference. Nucleotides were also characterized by ^{31}P NMR in D_2O using 85% H_3PO_4 as an external reference on a Bruker AC-200 spectrometer. Carbon assignments in nucleosides are based on hetero-nuclear multiple quantum correlation (HMQC) and hetero-nuclear multiple bond correlation (HMBC) experiments. COSY (correlated spectroscopy), HMQC, HMBC and NOESY (nuclear Overhauser effect spectroscopy) experiments were recorded on a Bruker DMX-600 spectrometer. Mass spectra were recorded on an AutoSpec-E-FISION VG high-resolution mass spectrometer. Nucleotides were characterized by FAB (fast atom bombardment) and high-resolution FAB using glycerol matrix under FAB negative conditions on an AutoSpec-E-FISION VG high-resolution mass spectrometer. Separation of the newly synthesized nucleotides was achieved on LC (Isco UA-6) using DEAE A-25 Sephadex (HCO_3-form) anion exchanger as described below. Final purification was performed on an HPLC (Merck-Hitachi) system using a semi-preparative LiChroCART LiChrospher 60 RP-select B column (1 × 25 cm; Merck KGaA) and a linear gradient of 0.1 M triethylammonium acetate buffer (TEAA, pH 7.5) and acetonitrile at 6 mL min^{-1} flow rate. The purity of the new nucleotides was evaluated on the same semi-preparative column, at 6 mL min^{-1}, in two different solvent systems. Solvent system I was 0.1 M TEAA–CH_3CN, 100 : 0 to 50 : 50 in 20 min. Solvent system II was 0.1 M TEAA–CH_3OH, 90 : 10 to 10 : 90 in 20 min. For the enzymatic assays a UV-2041 PC spectrophotometer (Shimadzu Co.) equipped with a Helma quartz cell type 9Q 10 was used.

Reagents

Ammonium sulfate, ATP, bovine serum albumin (BSA), calcium chloride, imidazole, malachite green, MES, tetramisole, thioglycollate and Tris-base were purchased from Sigma Chemical Co. (St. Louis, MO, USA). Bradford reagent was obtained from Bio-Rad Laboratories (Mississauga, Ont., Canada).

1-(3,5-Dimethylphenyl)-2,2,2-trifluoroethanone (9)

To a solution of 5-bromo-*m*-xylene (0.37 mL, 3.16 mmol) in dry ether (10 mL), n-butyllithium (1.6 M, 4 mL, 2 eq) was added at −30 °C under dry argon. The reaction mixture was allowed to warm up to 0 °C within 2.5 h and cooled down again to −50 °C. A solution of methyl trifluoroacetate (0.5 mL, 1.5 eq) in dry ether (0.5 mL) was added at −50 °C and the mixture was stirred for 3 h. The cooling bath was then removed and the mixture was hydrolyzed with saturated aqueous NH_4Cl. The organic phase was washed five times with aqueous NH_4Cl, three times with water, and dried over Na_2SO_4. The solvent was evaporated and the crude material was purified on an alumina gel (neutral) column eluted with petroleum ether till the impurity was removed, then the eluent was gradually changed to chloroform. The product was obtained as yellow oil in 91% yield (0.58 g). ^{1}H NMR ($CDCl_3$, 200 MHz) δ 7.70–7.64 (m, 2H, Ar), 7.36–7.30 (m, 1H, Ar), 2.40 (q, J = 0.5 Hz, 6H, CH_3); ^{13}C NMR ($CDCl_3$, 200 MHz) δ 180.8 (q, $^{2}J_{CF}$ = 35 Hz, *C*OCF_3), 138.9 (s, 2C, Ar), 137.3 (d, Ar), 130.1 (s, Ar), 127.8 (d, 2C, Ar), 116.8 (q, $^{1}J_{CF}$ = 291 Hz, CF_3), 21.2 (q, 2C, CH_3); ^{19}F NMR ($CDCl_3$, 200 MHz) δ −72.3 (s); MS (CI/CH_4) m/z 203 MH^+; high-resolution MS calcd for $C_{10}H_{10}F_3O$ 203.0684, found 203.0714.

1-(3,5-Dimethylphenyl)-2,2,2-trifluoroethanone oxime (10a)

A mixture of hydroxylamine hydrochloride (206 mg, 2.97 mmol) and NaOH (119 mg, 2.97 mmol) in absolute ethanol (10 mL) was heated under reflux. A solution of 5-(trifluoroacetyl)-*m*-xylene **9** (200 mg, 0.99 mmol) in absolute ethanol (1.5 mL) was added. After 22 h the solvent was evaporated under vacuum and the residue was partitioned between ether and water. The organic layer was washed three times with 0.01 M aqueous HCl, three times with water, and dried over Na_2SO_4. The solvent was removed to give the product as a cream solid (mp 97–98 °C) in 98% yield (213 mg). ^{1}H NMR ($CDCl_3$, 200 MHz) δ 9.04 (br s, 1H, NOH), 7.11 (br s, 3H, Ar), 2.36 (s, 3H, CH_3), 2.35 (s, 3H, CH_3); ^{13}C NMR ($CDCl_3$, 200 MHz) δ 148.1 (q, $^{2}J_{CF}$ = 32 Hz, *C*OCF_3), 138.3 (s, 2C, Ar), 132.3 (d, Ar), 126.1 (d, 2C, Ar), 125. 87 (s, Ar), 120.6 (q, $^{1}J_{CF}$ = 275 Hz, CF_3), 21.2 (q, 2C, CH_3); ^{19}F NMR ($CDCl_3$, 200 MHz) δ −68.0 (s); MS (CI/CH_4) m/z 218 MH^+; high-resolution MS calcd for $C_{10}H_{11}F_3NO$ 218.0793, found 218.0800.

N-(4-Toluenesulfonyl)-1-(3,5-dimethylphenyl)-2,2,2-trifluoroethanone oxime (10b)

Oxime **10a** (192 mg, 0.88 mmol) dissolved in 3 mL of dry pyridine was heated under reflux with *p*-toluenesulfonyl chloride (253 mg, 1.5 eq). After 3 h the solvent was removed under vacuum, and the residue was purified on an alumina (neutral) column (petroleum ether : chloroform 3 : 1). The product was obtained as a cream solid (mp 98–99 °C) in 88% yield (288 mg). ^{1}H NMR ($CDCl_3$, 200 MHz) δ 7.88 and 7.38 (AA′XX′, 2H each, Tos), 7.13 (br s, 1H, Ar), 6.95 (br s, 2H, Ar), 2.47 (s, 3H, Tos), 2.34 (s, 3H, CH_3), 2.33 (s, 3H, CH_3); ^{13}C NMR ($CDCl_3$, 300 MHz) δ 154.6 (q, $^{2}J_{CF}$ = 33 Hz, *C*OCF_3), 146.1 (s, Tos), 138.6 (s, 2C, Ar), 133.3 (d, Ar), 131.3 (s), 129.9 (d, 2C, Tos), 129.3 (d, 2C, Tos), 125.7 (d, 2C, Ar), 124.5 (s), 119.6 (q, $^{1}J_{CF}$ = 278 Hz, CF_3), 21.8 (q, Tos), 21.3 (q, 2C, CH_3); MS (CI/CH_4) m/z 372 MH^+; high-resolution MS calcd for $C_{17}H_{17}F_3NO_3S$ 372.0881, found 372.0858.

3-(3,5-Dimethylphenyl)-3-trifluoromethyldiaziridine (11)

A solution of **10b** (0.464 g, 1.25 mmol) in dry ether (5.5 mL), in a flame dried two necked flask, was cooled to −60 °C. Gaseous ammonia was liquified at −78 °C in a graded cylinder connected to the two neck flask. When the required amount of ammonia was accumulated (8 mL), the cooling bath was removed and gaseous ammonia was let into the reaction flask at −60 °C. The mixture was stirred for 8 h. The cooling bath was removed and ammonia was allowed to evaporate overnight. The residue was diluted with ether, washed with water, dried over Na_2SO_4, and the solvent was removed to give the product as a yellowish oil in 97% yield (0.261 g). The product was purified on a silica gel column and eluted with petroleum ether : chloroform 2 : 1. ^{1}H NMR ($CDCl_3$, 200 MHz) δ 7.20 (br s, 2H, Ar), 7.05 (br s, 1H, Ar), 2.75 (br s, 1H, NH), 2.32 (s, 6H, CH_3), 2.21 (br s, 1H, NH); ^{13}C NMR ($CDCl_3$, 300 MHz) δ 138.4 (s,

2C, Ar), 131.7 (d, Ar), 131.5 (s, Ar), 125.7 (d, 2C, Ar), 123.5 (q, $^1J_{CF}$ = 278 Hz, CF_3), 58.0 (q, $^2J_{CF}$ = 36 Hz, C-diaziridine), 21.1 (q, 2C, CH_3); ^{19}F NMR ($CDCl_3$, 200 MHz) δ −76.7 (s); MS (CI/CH_4) *m*/*z* 217 MH^+; high-resolution MS calcd for $C_{10}H_{12}F_3N_2$ 217.0953, found 217.0948.

3-[3,5-Bis(bromomethyl)phenyl]-3-trifluoromethyl-3*H*-diazirine (5a)

Compound **11** (0.247 g, 1.14 mmol) was dissolved in methyl formate (10 mL). *N*-Bromosuccinimide (NBS) (611 mg, 3 eq) and dibenzoyl peroxide (55 mg, 0.2 eq) were added. The reaction was heated under reflux overnight under the light of four fluorescent PL 11W lamps (or under sunlight for 8 h). TLC on a silica gel plate, using petroleum ether : chloroform 2 : 1, indicated the disappearance of the starting material (R_f = 0 pink spot with ninhydrin spray) and the formation of two products: 3-(3-methyl-5-bromomethylphenyl)-3-trifluoromethyl-3*H*-diazirine (**5b**) (R_f 0.54) and 3-[3,5-bis(bromomethyl)phenyl]-3-trifluoromethyl-3*H*-diazirine (**5a**) as a minor product (R_f 0.43) in a ratio of 2 : 1, respectively. Both products were not colored with ninhydrin spray. The desired product was purified on a silica gel column eluted with petroleum ether. Compound **5a** was obtained in 24% yield as colorless oil. ^{1}H NMR ($CDCl_3$, 200 MHz) δ 7.48 (t, *J* = 1.5 Hz, 1H, Ar), 7.13 (br s, 2H, Ar), 4.44 (s, 4H, CH_2Br); ^{13}C NMR ($CDCl_3$, 300 MHz) δ 140.0 (s, 2C, Ar), 130.9 (d, Ar), 130.5 (s, Ar), 126.9 (d, 2CH, Ar), 121.9 (q, $^1J_{CF}$ = 275 Hz, CF_3), 31.5 (t, $2CH_2Br$), 28.2 (q, $^2J_{CF}$ = 40 Hz, C-diazirine); UV λ_{max} ($CHCl_3$)/nm 353. **5b** obtained in 51% yield as colorless oil. ^{1}H NMR ($CDCl_3$, 200 MHz) δ 7.26 (br s, 1H, Ar), 6.99 (br s, 1H, Ar), 6.93 (br s, 1H, Ar), 4.41 (s, 2H, CH_2Br), 2.35 (s, 3H, CH_3); ^{13}C NMR ($CDCl_3$, 300 MHz) δ 139.6 (s, Ar), 138.6 (s, Ar), 131.1 (d, Ar), 129.7 (s, Ar), 127.1 (d, Ar), 124.1 (d, Ar), 122.0 (q, $^1J_{CF}$ = 275 Hz, CF_3), 32.3 (t, CH_2Br), 28.2 (q, $^2J_{CF}$ = 40 Hz, C-diazirine), 21.3 (q, CH_3); UV λ_{max} ($CHCl_3$)/nm 353. Compound **5b** was recycled and brominated again. The reaction was carried out on 0.85 mmol of **5b** by the above procedure using only 1 eq of NBS. Product **5a** was obtained in 64% yield (202 mg).

5-{6-Amino-8-[3-bromomethyl-5-(3-trifluoromethyl-3*H*-diazirin-3-yl)benzylsulfanyl]purin-9-yl}-2-hydroxymethyltetrahydrofuran-3,4-diol (13)

Adenosine 8-thiolate sodium salt (0.14 mmol) was dissolved in dry DMF (10 mL) and compound **5a** (109 mg, 2 eq) dissolved in DMF (2 mL) was added. The solution was stirred under nitrogen at room temperature for 4 h. The solvent was evaporated under vacuum and the residue was co-evaporated repeatedly with EtOH until it turned into a yellow solid. The product was purified on a silica gel column eluted with chloroform : methanol 15 : 1. After evaporation and drying for two days *in vacuo* the product was obtained in 60% yield (50 mg). ^{1}H NMR (CD_3OD, 200 MHz) δ 8.08 (s, 1H, H-2), 7.60 (br s, 1H, Ar), 7.21 (br s, 1H, Ar), 7.16 (br s, 1H, Ar), 5.96 (d, *J* = 7 Hz, 1H, H-1′), 4.98 (dd, *J* = 7, 5 Hz, 1H, H-2′), 4.60 and 4.44 (Abq, *J* = 12 Hz, 2H, CH_2S), 4.51 (s, 2H, CH_2Br), 4.33 (dd, *J* = 5, 1.5 Hz, 1H, H-3′), 4.19–4.13 (m, 1H, H-4′), 3.87 (dd, *J* = 12.5, 2 Hz, 1H, H-5′), 3.71 (dd, *J* = 12.5, 2.5 Hz, 1H, H-5′); ^{13}C NMR (CD_3OD, 300 MHz) δ 156.2 (s, C-6), 152.4 (d, C-2), 151.4 (s, C-4), 149.8 (s, C-8), 141.29 (s, Ar), 140.5 (s, Ar), 132.6 (d, Ar), 130.7 (s, Ar), 128.0 (d, Ar), 127.2 (d, Ar), 123.3 (q, $^1J_{CF}$ = 275 Hz, CF_3), 121.3 (s, C-5), 91.3 (d, C-1′), 88.8 (s, C-4′), 74.1 (d, C-2′), 73.0 (d, C-3′), 64.0 (t, C-5′), 37.5 (d), 32.4 (d), 29.3 (q, $^2J_{CF}$ = 40 Hz, C-diazirine).

N-(2-{2-[3-[6-Amino-9-(3,4-dihydroxy-5-hydroxymethyltetrahydrofuran-2-yl)-9*H*-purin-8-ylsulfanylmethyl]-5-(3-trifluoromethyl-3*H*-diazirin-3-yl)benzylamino]ethyldisulfanyl}ethyl)-carbamic acid *tert*-butyl ester (15)

N-(*tert*-Butyloxycarbonyl)cystamine[44] (250 mg, 5 eq) and Dowex-MWA-1 (57 mg) were added to **13** (117 mg, 0.198 mmol) in DMF (5 mL). The reaction was stirred under nitrogen at 60 °C for 6 h. Dowex-MWA-1 was removed by filtration. The solvent was evaporated under vacuum and the residue was co-evaporated repeatedly with EtOH. The product was purified on a silica gel column eluted with chloroform : methanol 15 : 1. After evaporation and drying for two days under vacuum the product was obtained in 48% yield (73 mg). ^{1}H NMR (CD_3OD, 200 MHz) δ 8.08 (s, 1H, H-2), 7.57 (br s, 1H, Ar), 7.20 (br s, 1H, Ar), 7.11 (br s, 1H, Ar), 5.94 (d, *J* = 7 Hz, 1H, H-1′), 4.95 (dd, *J* = 7, 5 Hz, 1H, H-2′), 4.64 and 4.45 (Abq, *J* = 8 Hz, 2H, CH_2S), 4.32 (dd, *J* = 5, 1.5 Hz, 1H, H-3′), 4.19–4.09 (m, 1H, H-4′), 3.86 (dd, *J* = 12, 2 Hz, 1H, H-5′), 3.75 (s, 2H, Ar-CH_2NH), 3.69 (dd, *J* = 12, 3 Hz, 1H, H-5′), 3.30 (t, *J* = 7 Hz, 2H, CH_2NH), 2.79 (br s, 4H, CH_2SSCH_2), 2.71 (t, *J* = 7 Hz, 2H, CH_2NHCO), 1.42 (s, 9H, Boc); ^{13}C NMR (CD_3OD, 300 MHz) δ 158.3 (s, Boc), 156.3 (s, C-6), 152.5 (d, C-2), 151.5 (s, C-4), 150.1 (s, C-8), 142.5 (s, Ar), 140.2 (s, Ar), 132.1 (d, Ar), 130.5 (s, Ar), 127.2 (d, Ar), 126.8 (d, Ar), 123.5 (q, $^1J_{CF}$ = 275 Hz, CF_3), 121.4 (s, C-5), 91.4 (d, C-1′), 88.9 (s, C-4′), 80.2 (s, Boc), 74.2 (d, C-2′), 73.1 (d, C-3′), 64.1 (t, C-5′), 53.3 (d), 48.1 (d), 40.7 (d), 39.1 (d), 38.7 (d), 37.7 (d), 29.4 (q, $^2J_{CF}$ = 40 Hz, C-diazirine).

N-(2-{2-[3-[6-Amino-9-(3,4-dihydroxy-5-phosphonooxymethyltetrahydrofuran-2-yl)-9*H*-purin-8-ylsulfanylmethyl]-5-(3-trifluoromethyl-3*H*-diazirin-3-yl)benzylamino]ethyldisulfanyl}ethyl)carbamic acid *tert*-butyl ester (16)

A solution of nucleoside **15** (30 mg, 0.039 mmol) in dry trimethyl phosphate (1 mL) was added to a flame-dried flask under nitrogen. The solution was cooled to 0 °C, then proton sponge (13 mg, 2 eq) was added. After 20 min, distilled phosphorous oxychloride (8.4 µL, 3 eq) was added dropwise and a purple clear solution was formed. Stirring was continued for 2 h at 0 °C. TLC (1-propanol–28% NH_4OH–H_2O (11 : 2 : 7)), indicated the disappearance of starting material and formation of a polar product (R_f 0.39). 0.2 M TEAB solution (10 mL) was added. Stirring continued for 45 min and then the solution was freeze-dried. The residue was separated on HPLC applying a linear gradient of TEAA–CH_3CN 100 : 0 to 50 : 50 in 20 min followed by isocratic elution for 5 min (TEAA–CH_3CN, 50 : 50, 6 mL min^{-1}) t_R 19.48 min. The product was obtained as a white solid in 31% yield (12 mg). ^{1}H NMR (D_2O, 200 MHz) δ 8.10 (s, 1H, H-2), 7.61 (br s, 1H, Ar), 7.26 (br s, 1H, Ar), 7.12 (br s, 1H, Ar), 6.09 (d, *J* = 6 Hz, 1H, H-1′), (H-2′ is hidden by the water peak), 4.55–4.32 (m, 2H, CH_2S), 4.31–3.87 (m, 6H, H-3′, H-4′, H-5′ & Ar-CH_2-NH), 3.30–3.07 (m, 4H, CH_2NH and CH_2-NHCO), 2.74–2.38 (m, 4H, CH_2SSCH_2), 1.35 (s, 9H, Boc); ^{31}P NMR (D_2O, 200 MHz, pH 5) δ 4.2 (s); FAB (negative) 839 (M^{2-}), 841 (M^{2-} + $2H^+$). High-resolution FAB calc for $C_{29}H_{39}N_9O_9F_3PS$ 841.1722, found 841.1670; t_R 19.21 min (90% purity) using solvent system I, 21.60 min (92% purity) using solvent system II.

N-(2-{2-[3-[6-Amino-9-(3,4-dihydroxy-5-(phosphonooxy-phosphonooxyphosphonooxymethyl)tetrahydrofuran-2-yl)-9*H*-purin-8-ylsulfanylmethyl]-5-(3-trifluoromethyl-3*H*-diazirin-3-yl)-benzylamino]ethyldisulfanyl}ethyl)carbamic acid *tert*-butyl ester (17)

CDI (22 mg, 0.13 mmol) was added to a flame-dried flask under nitrogen containing nucleotide **16** (22 mg, 0.022 mmol) in dry DMF (1 mL). The solution was stirred under nitrogen at room temperature for 4 h. TLC (isopropanol–28% NH_4OH–H_2O (6 : 3 : 1), indicated the disappearance of starting material. Dry methanol (8 µL) was then added to the reaction mixture. After 5 min 0.1 M $(Bu_3NH)_4P_2O_7$ in DMF (110 mL), prepared from $Na_2H_4P_2O_7$ with 4 eq of Bu_3N in 0 °C, was added at once and the mixture was stirred under nitrogen at room temperature for 3 h. TLC (isopropanol–28% NH_4OH–H_2O (6 : 3 : 1), indicated the disappearance of starting material and formation of product **17** (R_f 0.46). The solvent was evaporated under vacuum.

The crude residue was separated on HPLC applying a linear gradient of TEAA–CH_3CN 100 : 0 to 50 : 50 in 20 min followed by isocratic elution for 5 min (TEAA–CH_3CN, 50 : 50, 6 mL min^{-1}) t_R 17.41 min. The product was obtained as a white solid in 19% yield (4.6 mg). ^1H NMR (D_2O, 600 MHz) δ 8.13 (s, 1H, H-2), 7.32 (br s, 1H, Ar), 7.27 (br s, 1H, Ar), 7.09 (br s, 1H, Ar), 6.16 (d, J = 6 Hz, 1H, H-1′), 5.17 (t, J = 6 Hz, 1H, H-2′), 5.09–4.96 (m, 1H, H-3′), 4.65–4.45 (m, 2H, CH_2S), 4.44–4.25 (m, 5H, H-4′, H-5′ and Ar-CH_2-NH), 3.56–2.98 (m, 4H, CH_2NH and CH_2NHCO), 2.68–2.41 (m, 4H, CH_2SSCH_2), 1.35 (s, 9H, Boc); ^{31}P NMR (D_2O, 200 MHz, pH 8) δ −9.1 (d), −10.7 (d), −22.0 (t).

2-{2-[3-[6-Amino-9-(3,4-dihydroxy-5-(phosphonooxyphosphonooxyphosphonooxymethyl)tetrahydrofuran-2-yl)-9*H*-purin-8-ylsulfanylmethyl]-5-(3-trifluoromethyl-3*H*-diazirin-3-yl)benzylamino]ethyldisulfanyl}ethylamine (19)

Nucleotide **17** (4.6 mg, 0.0042 mmol) was dissolved in neat TFA (2 mL) and the solution was stirred at room temperature for 3 min. Then, TFA was evaporated by air flow for an additional 3 min. Product **19** was purified on HPLC applying a linear gradient of TEAA–CH_3CN 100 : 0 to 50 : 50 in 20 min followed then by an isocratic elution for 5 min (TEAA–CH_3CN, 50 : 50) at 6 mL min^{-1}, t_R 13.98 min. The product was obtained as a white solid, in a quantitative yield (4.3 mg). ^1H NMR (D_2O, 600 MHz) δ 8.20 (s, 1H, H-2), 7.35 (br s, 1H, Ar), 7.32 (br s, 1H, Ar), 7.12 (br s, 1H, Ar), 6.20 (d, J = 6 Hz, 1H, H-1′), 5.17–5.26 (m, 1H, H-2′), 5.14–5.09 (m, 1H, H-3′), 4.66–4.52 (m, 2H, CH_2S), 4.51–4.24 (m, 5H, H-4′, H-5′ and Ar-CH_2-NH), 3.53–3.02 (m, 4H, CH_2NH and CH_2NHCO), 2.85–2.70 (m, 2H, CH_2SSCH_2), 2.67–2.5 (m, 2H, CH_2SSCH_2); ^{31}P NMR (D_2O, 200 MHz, pH 8) δ −7.6 (d), −10.7 (d), −21.0 (t); UV λ_{max} (H_2O)/nm 285, 353; t_R 13.10 min (92% purity) using solvent system I, 14.03 min (93% purity) using solvent system II. FAB (negative, glycerol) 923 ($M^{2-} - 2H^+ + 2Na^+$).

Product **18** was obtained in the same way in 100% yield starting from 3.9 mg (0.0037 mmol) nucleotide **16**. ^1H NMR (D_2O, 200 MHz) δ 8.19 (s, 1H, H-2), 7.61 (br s, 1H, Ar), 7.23 (br s, 1H, Ar), 7.21 (br s, 1H, Ar), 6.01 (d, J = 6 Hz, 1H, H-1′), 4.87 (t, J = 6, 1H, H-2′), 4.52–4.38 (m, 2H, CH_2S), 4.29–4.04 (m, 6H, H-3′, H-4′, H-5′ and Ar-CH_2-NH), 3.31–3.09 (m, 4H, CH_2NH and CH_2NHCO), 2.86–2.74 (m, 4H, CH_2SSCH_2); ^{31}P NMR (D_2O, 200 MHz, pH 8) δ 1.1 (s); UV λ_{max} (H_2O)/nm 285, 353; FAB (negative, glycerol) 741 $(M - H)^-$, 740 $(M - 2H)^-$.

Coupling nucleotides 18 or 19 to magnetic microspheres

Nucleotide **19** (1.9 mg, 0.0017 mmol) was dissolved in 0.1 M ammonium bicarbonate buffer, pH 8.3 (1 mL), and magnetic microspheres, **6** (1 mg), were added. The reaction mixture was shaken at room temperature overnight. Magnetic microspheres were separated from the solution by a strong magnet and washed with 0.1 M ammonium bicarbonate buffer (4 mL). The amount of the remaining nucleotide **19** was established based on the absorption of the filtrate at 285 nm. Finally, the number of moles of **19** connected to the magnetic microspheres was calculated. PALMm product **2** was obtained in 70% yield.

PALMm product **1** was obtained in the same way in 74% yield starting from 12 mg (0.0019 mmol) compound **18**.

Synthesis of functional magnetic polystyrene–silica hybrid microspheres 6

1) Monodispersed polystyrene microspheres were prepared according to the literature.[56] In a typical experiment, polystyrene microspheres of 4.5 μm median size diameter (SD 0.07 μm) were formed by introducing into a reaction flask (1 L) a solution containing PVP, MW 360 000 (1.25 g, 0.5% w/v of total solution) dissolved in a mixture of EtOH (150 mL) and 2-methoxyethanol (62.5 mL). The temperature of the mechanically stirred solution was then preset to 73 °C. Nitrogen was bubbled through the solution for *ca.* 15 min to exclude air, and then a blanket of nitrogen was maintained over the solution during the polymerization period. A deaerated solution containing the initiator benzoyl peroxide (1.5 g, 0.6% w/v of total solution) and styrene (37.5 mL, 16% w/v of total solution) was then added to the reaction flask. The polymerization reaction continued for 24 h and was then stopped by cooling. The microspheres formed were washed by extensive centrifugation cycles with EtOH and then with water. The particles were then dried by lyophilization.

2) Magnetic polystyrene microspheres were formed by seeded polymerization of iron salts on the former polystyrene microspheres according to the literature.[40b] In a typical experiment, polystyrene microspheres (2.3 μm, 1 g) were added to a flask containing 20 mL distilled water. The formed mixture was sonicated for a few minutes and then mechanically stirred at *ca.* 200 rpm. The temperature was then preset to 60 °C. Nitrogen was bubbled through the suspension during the coating process to exclude air. 0.1 mL of iron chloride tetrahydrate aqueous solution (1.2 mmol in 10 mL H_2O) and 0.1 mL of $NaNO_2$ aqueous solution (0.02 mmol in 10 mL H_2O) were then successively introduced into the reaction flask. Thereafter, NaOH aqueous solution (0.5 mmol in 10 mL H_2O) was added until a pH of *ca.* 10 was reached. This procedure was repeated four times. During this coating process the microspheres became brown–black colored. The suspension was then cooled to room temperature. The formed magnetic polystyrene microspheres were then washed extensively in water with a magnet and dried in a vacuum oven.

3) Silica microspheres of substantially smaller size (30–40 nm) were coated on the magnetic polystyrene microspheres by seeded polymerization of tetraethoxysilane on the surface of these particles, according to the Stober method.[40b,57] In a typical experiment, magnetic polystyrene microspheres (2.3 μm, 1 g) were added to a flask containing EtOH (93.6 mL) and distilled water (1.9 mL), and the mixture was sonicated to disperse the particles. Ammonium hydroxide (1.3 mL) and $Si(OEt)_4$ (3.2 mL) were then added, and the resulting suspension was shaken at room temperature for 12 h. The resulting magnetic polystyrene microspheres coated with silica nanoparticles were freed from free silica particles (30–40 nm diameter) by repeated centrifugation cycles. The magnetic polystyrene–silica microspheres were then dried in a vacuum oven.

4) Magnetic polystyrene–silica microspheres containing amine groups were prepared by reacting these particles with $Si(OEt)_3(CH_2)_3NH_2$, according to the literature.[58] In a typical experiment, $Si(OEt)_3(CH_2)_3NH_2$ (8 mL) was added into a flask containing 1 g of monodispersed silica coated microspheres of 2.3 μm average diameter dispersed in 100 mL buffer acetate, 0.1 M at pH 5.5. The suspension was stirred at 60 °C for 18 h. Thereafter, the amino derivatized microspheres were washed intensively by several centrifugation cycles with buffer acetate and distilled water, respectively and dried in a vacuum oven.

5) The amino derivatized microspheres (10 mg) were shaken in 0.1 M $NaHCO_3$, pH 8.5, 1 mL, and treated with divinyl sulfone (1 mg), at room temperature for 4 h. The particles were collected with a magnet, washed several times, and freeze dried. The diameter of microspheres **6** was 5.5 ± 15% micron.

Characterization of the magnetic microspheres 6

Mercaptoethanol (11.5 μL, 0.16 mmol) was dissolved in 0.1 M sodium bicarbonate buffer (1.5 mL), pH 8.5, and magnetic microspheres **6** (10 mg) were added. The reaction mixture was shaken at room temperature overnight. The magnetic microspheres were filtered and 4.6 μL of the filtrate was diluted in 0.1 M sodium bicarbonate buffer (1.5 mL) and added to the solution of 4,4′-dipyridyl disulfide (4-PDS) (0.66 mg, 0.003 mmol) in 0.1 M sodium bicarbonate buffer, pH 8.5 (1.5 mL).

The reaction was stirred at room temperature for 5 min and the absorbance of the final solution was measured at 321 nm. Finally, the number of free binding sites on the microspheres was calculated.

Evaluation of 8-BuS-ATP as a hexokinase substrate

The assay was conducted according to the Sigma quality control test procedure. Hexokinase used for this assay is from *Saccharomyces cerevisiae* (Sigma Co). Fresh 8-BuS-ATP solution (19 mM) was used. 8-BuS-ATP concentration in the assay solution was 370 μM. The assay was performed in duplicate (SEM 0.013).

Evaluation of 8-BuS-ATP and 8-BuS-AMP as hexokinase inhibitors

Freshly prepared 8-BuS-ATP, 8-BuS-AMP, and ATP solutions, each at 19 mM concentration, were used. The resulting activity of the enzyme was compared to that with ATP alone. 8-BuS-ATP, 8-BuS-AMP, and ATP concentrations in the assay solution were 370 μM for each.

Evaluation of PALM reagent 2 as a hexokinase substrate or inhibitor

A freshly prepared solution of PALMm reagent **2** was used. Reagents were added according to the standard assay, and the final solution was immediately mixed by inversion and the increase in absorbance, at 340 nm, was recorded for 20 min. The assay was done in duplicate. Calculations of enzyme activity used absorbance data from the fifth minute onwards, after the magnetic microspheres had completely sank down. PALMm reagent **2** at 890 μM reduced hexokinase activity to 23% compared to ATP.

In the same way, PALMm reagent **2** was evaluated as hexokinase inhibitor at 1.26 mM concentration, in the presence of ATP (1.26 mM). The resulting activity of the enzyme was compared to that with ATP alone (1.26 mM). Reagent **2** had no inhibitory effect.

NTPDase assays

Enzyme activity was measured by the release of inorganic phosphate with the malachite green colorimetric assay.[52] Activity was determined at 37 °C (NTPDase1) or 30 °C (apyrase) in 1 mL of the following incubation medium: 8 mM $CaCl_2$, 5 mM tetramisole, 50 mM imidazole, and 50 mM Tris-base buffered at pH 7.5, as described before.[59] The enzyme preparation (1.1 μg), NTPDase1 consisting of a bovine spleen particulate fraction, isolated as previously described,[59] or potato apyrase, purified as described below, was added to the incubation medium and pre-incubated for 3 min (NTPDase1) or 2 min (apyrase). The reaction of the enzyme was started by adding 100 μM of ATP in the presence of different concentrations of either 8-BuS-AMP or analogue **16**, and stopped 7 min later with 250 μL of the malachite green reagent. Similarly, the reaction of apyrase was started by adding 1.26 mM ATP to a 1.26 mM PALMm reagent **1** solution and the reaction was stopped after 15 min. Controls (with the same concentrations of ATP) were run in parallel by adding the enzyme after the malachite green reagent. Enzyme hydrolysis was expressed as units, *i.e.*, micromoles of Pi released per minute per milligram of protein (μmol min^{-1} mg^{-1}).[28] Protein concentration was estimated by the Bradford microplate assay, using bovine serum albumin as a reference standard.[60] Results are the mean of triplicate or duplicate samples. The maximum deviation from the mean was within 10%.

Potato (*Solanum tuberosum*) apyrase purification

All steps were carried out at 4 °C unless stated otherwise. Soluble apyrase was purified from potatoes *(Solanum tuberosum* Idaho) as described before.[61] Briefly, potatoes (5 kg) were peeled, diced and homogenized in an ice cold solution of thioglycollate (50 mM) corresponding to half the volume of potato (2.5 L per 5 Kg). This homogenate was agitated for 15 min, filtered through 8 layers of cheesecloth and the turbid extract was centrifuged 10 min at 1000*g* to eliminate a solid white precipitate, then centrifuged a second time 15 min at 13 000*g* to eliminate cell debris. Two consecutive salting-outs in 40% and 70% of ammonium sulfate saturation were performed, the pH was adjusted to pH 4.0. The extract was filtered through 3–4 layers of cheesecloth, then centrifuged 15 min at 13 000*g*. The final pellet was re-suspended in 2% of initial potato volume. The enriched fraction obtained (≈110 mg protein) was applied to an affinity column (5.8 ml of Cibacron blue F3G-A, BioRad Inc., Hercules, CA, USA) previously rinsed with at least 5 volumes of washing buffer (MES 100 mM, NaCl 0.5 M, pH 6.0). The fraction was put three times on the column for maximum adsorption, then washed 5 times with washing buffer. The enzyme was eluted by a linear gradient (0.5–4 M) of NaCl. 1 mL sample were collected and fractions containing activity were pooled and concentrated using Centriprep30 (AMICON). The concentrate was centrifuged 15 min at 13 000*g* then applied to a Sephadex 75 HR 10/30 column (10 × 300 mm), previously rinsed with 4 volumes of elution buffer (MES 100 mM, pH 6.0). 2 mL was injected in the injection loop of an ÄKTAexplorer (Amersham Pharmacia Biotech, Baie d′Urfé, Qc, Canada) and 1 mL samples were collected. Fractions containing more then 20% of total activity were pooled.

Acknowledgements

This work was supported in part by the Marcus Center for Medicinal Chemistry.

References

1 (*a*) F. Kotzyba-Hibert, I. Kapfer and M. Goeldner, *Angew. Chem., Int. Ed. Engl.*, 1995, **34**, 1296–1312; (*b*) S. A. Fleming, *Tetrahedron*, 1995, **51**, 12479–12520; (*c*) M. S. Platz, *Photochem. Photobiol.*, 1997, **65**, 193–194; (*d*) G. Dorman and G. D. Pretwich, *Trends Biotechnol.*, 2000, **18**, 64–77; (*e*) G. A. Kurshunova, N. V. Sumbatyan, A. N. Topin and M. T. Mtchedlidze, *Mol. Biol. (Engl. Transl.)*, 2000, **34**, 823–839; (*f*) Y. Hatanaka and Y. Sadakane, *Curr. Top. Med. Chem.*, 2002, **2**, 271–288.
2 (*a*) J. Brunner, H. Senn and F. M. Richards, *J. Biol. Chem.*, 1980, **255**, 3313–3318; (*b*) T. Nakayama and H. G. Khorana, *J. Biol. Chem.*, 1990, **265**, 15762–15769.
3 (*a*) S. X. Cai, D. J. Glenn and J. F. W. Kenea, *J. Org. Chem.*, 1992, **57**, 1299–1304; (*b*) I. Kapfer, J. E. Hawkinson, J. E. Casida and M. P. Goeldner, *J. Med. Chem.*, 1994, **37**, 133–140.
4 F. Hucho and C. Weise, *Angew. Chem., Int. Ed.*, 2001, **40**, 3100–3116.
5 S. M. Parsons, *FASEB J.*, 2000, **14**, 2423–2434.
6 A. Favre, C. Saintome, J.-L. Fourrey, C. Pascale and L. J. Philippe, *Photochem. Photobiol.*, 1998, **42**, 109–124.
7 G. Dorman, *Top. Curr. Chem.*, 2001, **211**, 169–225.
8 (*a*) M. C. Olcott, M. L. Bradley and B. E. Haley, *Biochemistry*, 1994, **33**, 11935–11941; (*b*) J. Kanaani, D. Maltby, P. Focia and C. C. Wang, *Biochemistry*, 1995, **34**, 14987–14996; (*c*) D. Tull, S. Miao, S. G. Withers and R. Aebersold, *Anal. Biochem.*, 1995, **224**, 509–514; (*d*) R. A. Tschirret-Guth, K. F. Medzihiradszky and P. R. Oritz de Montellano, *J. Am. Chem. Soc.*, 1998, **120**, 7404–7410.
9 Y. Hatanaka, M. Hashimoto and Y. Kanaoka, *J. Am. Chem. Soc.*, 1998, **120**, 453–454.
10 K. Muramoto and H. Kamiya, *Dev. Comp. Immunol.*, 1992, **16**, 1–8.
11 H-J. Schafer, P. Scheurich, G. Rathgerber and K. Dose, *Anal. Biochem.*, 1980, **104**, 106–111.
12 (*a*) K. Fang, M. Hashimoto, S. Jokusch, N. J. Turro and K. Nakanishi, *J. Am. Chem. Soc.*, 1998, **120**, 8543–8544; (*b*) L. Hong-yu, Y. Liu, K. Fang and K. Nakanishi, *Chem. Commun.*, 1999, 365–366.
13 A. M. Mulichak, J. E. Wilson, K. Padmanabhan and R. M. Garavito, *Nat. Struct. Biol.*, 1998, **5**, 555–560.
14 C. Zeng and H. J. Fromm, *J. Biol. Chem.*, 1995, **270**, 10509–10513.
15 W. S. Bennett and T. A. Steitz, *J. Mol. Biol.*, 1980, **140**, 211–230.

16 A. E. Aleshin, C. Zeng, H. D. Bartunik, H. J. Fromm and R. B. Honzatko, *J. Mol. Biol.*, 1998, **282**, 345–357.
17 X. Liu, C. S. Kim, F. T. Kurbanov, R. B. Honzatko and H. J. Fromm, *J. Biol. Chem.*, 1999, **274**, 31155–31159.
18 (*a*) G. Burnstock, *Pharmacol. Rev.*, 1972, **24**, 509–81; (*b*) G. Burnstock, *J. Theor. Biol.*, 1976, **62**, 491–503.
19 I. Kugelgen and A. Wetter, *Naunyn-Schmiedeberg's Arch. Pharmacol.*, 2000, **362**, 310–323.
20 (*a*) B. F. King, A. Townsend-Nicholson and G. Burnstock, *Trends Pharmacol. Sci.*, 1998, **19**, 506–514; (*b*) F. D. Virgillo, P. Chiozzi, D. Ferrari, S. Falzoni, J. M. Sanz, A. Morelli, M. Torboli, G. Bolognesi and O. R. Baricordi, *Blood*, 2001, **97**, 587–600.
21 (*a*) H. P. Baer and G. I. Drummond, *Physiological and Regulatory Functions of Adenosine and Adenine Nucleotides*, Raven Press, New York 1979; (*b*) M. Williams, *Annu. Rev. Pharmacol. Toxicol.*, 1987, **27**, 315–45.
22 E. A. Barnard, J. Simon and T. E. Webb, *Mol. Neurobiol.*, 1997, **15**, 103–129.
23 M. R. Boarder and S. M. O. Hourani, *Trends Pharmacol. Sci.*, 1998, **19**, 99–107.
24 (*a*) R. A. Olsson and J. D. Pearson, *Physiol. Rev.*, 1990, **70**, 761–845; (*b*) T. W. Stone and H. A. Simmonds, *Purines: Basic and Clinical Aspects*, Kluwer Academic Publishers, 1991, pp. 1–245.
25 (*a*) B. Fischer, *Exp. Opin. Ther. Pat.*, 1999, **9**, 385–399; (*b*) K. Inoue, *Pharmacol. Res.*, 1998, **38**, 323–331; (*c*) M. P. Abbrachio, *Drug Dev. Res.*, 1996, **39**, 393–406; (*d*) C. M. Chan, R. J. Unwin and G. Burnstock, *Exp. Nephrol.*, 1998, **6**, 200–207; (*e*) T. D. White, *Pharmacol. Ther.*, 1988, **38**, 129–68.
26 C. C. Caldwell, M. D. Davis and A. F. Knowles, *Arch. Biochem. Biophys.*, 1999, **362**, 46–58.
27 (*a*) K. Enjyoji, J. Sevigny, Y. Lin, P. S. Fenette, P. D. Christie, J. Schulteam Esch II, M. Imai, J. M. Edelberg, H. Rayburn, M. Lecht, D. L. Beller, E. Csizmadia, D. D. Wagner, S. C. Robson and R. D. Rosenburg, *Nat. Med.*, 1999, **5**, 101–1017; (*b*) C. Goepfert, C. Sundberg, J. Sévigny, K. Enjyoji, T. Hoshi, E. Csizmadia and S. C. Robson, *Circulation*, 2001, **104**, 3109–15; (*c*) N. Mizumoto, T. Kumamoto, S. C. Robson, J. Sévigny, H. Matsue, K. Enjyoji and A. Takashima, *Nat. Med.*, 2002, **8**, 358–365.
28 D. Lebel, G. G. Poirier, S. Phaneuf, P. St Jean, J. F. Laliberte and A. R. Beaudoin, *J. Biol. Chem.*, 1980, **255**, 1227–1233.
29 J.-F. Laliberté, P. St-Jean and A. R. Beaudoin, *J. Biol. Chem.*, 1982, **257**, 3869–3874.
30 Y. Côté, P. St-Jean, R. Béliveau, M. Potier and A. R. Beaudoin, *Biochim. Biophys. Acta*, 1991, **1078**, 87–191.
31 (*a*) R. Lemmens, L. Vanduffel, A. Kittel, A. R. Beaudoin, O. Benrezzak and J. Sevigny, *Eur. J. Biochem.*, 2000, **267**, 4106–4114; (*b*) E. J. Schulte Am, J. Sevigny, E. Kaczmarek, J. B. Siegel, M. Imai, K. Koziak, A. R. Beaudoin and S. C. Robson, *Biochemistry*, 1999, **38**, 2248–2258.
32 T. M. Smith and T. L. Kirley, *Biochemistry*, 1999, **38**, 321–328.
33 (*a*) S. C. Robson, S. Daoud, M. Bégin, Y. P. Côté, J. B. Siegel, F. H. Bach and A. R. Beaudoin, *Blood Coagulation Fibrinolysis*, 1997, **8**, 21–27; (*b*) T. F. Wang, Y. Ou and G. Guidotti, *J. Biol. Chem.*, 1998, **273**, 24814–24821; (*c*) A. Grinthal and G. Guidotti, *Biochemisty*, 2002, **41**, 1947–1956.
34 (*a*) G. V. R. Born, *Nature*, 1962, **194**, 927–929; (*b*) H. Zimmermann, *Nat. Med.*, 1999, **5**, 987–988; (*c*) A. J. Marcus, M. J. Broekman, J. H. F. Drosopoulos, N. Islam, T. N. Alyonycheva, L. B. Safier, K. A. Hajjar, D. N. Posnett, M. A. Schoenborn, K. A. Schooley, R. B. Gayle and C. R. Maliszewski, *J. Clin. Invest.*, 1997, **99**, 1351–1360; (*d*) A. J. Marcus and L. B. Safier, *FASEB J.*, 1993, **7**, 516–522; (*e*) A. R. Beaudoin, J. Sévigny, F. P. Gendron, M. St-Georges, M. C. Leclerc, in *Emerging Therapeutic Targets*, ed. A. Ward, Ashley Publications Ltd, 1998, Vol. II.
35 F. P. Gendron, E. Halbfinger, B. Fischer, M. Duval, P. D'Orléans-Juste and A. R. Beaudoin, *J. Med. Chem.*, 2000, **43**, 2239–2247.
36 E. Halbfinger, D. T. Major, M. Ritzmann, J. Ubl, G. Reiser, J. L. Boyer, K. T. Harden and B. Fischer, *J. Med. Chem.*, 1999, **42**, 5325–5337.
37 (*a*) J. Brunner, *Ann. Rev. Biochem.*, 1993, **62**, 483–514; (*b*) Y. Hatanaka, H. Nakayama and Y. Kanaoka, *Rev. Heteroat. Chem.*, 1996, **14**, 213–243; (*c*) Y. Hatanaka, M. Hashimoto, H. Nakayama, Y. Kanaoka, L. Sun and H. D. Showalter, *Chemtracts: Org. Chem.*, 1994, **7**, 235–237.
38 Y. Hatanaka, E. Yoshida, H. Nakayama and Y. Kanaoka, *Bioorg. Chem.*, 1989, **17**, 482–485.
39 (*a*) J. A. Burns, J. C. Butler, J. Moran and G. M. Whitesides, *J. Org. Chem.*, 1991, **56**, 2648–2650; (*b*) J. C. Han and G. Y. Han, *Anal. Biochem.*, 1994, **220**, 5–10.
40 (*a*) S. Margel, S. Gura, H. Bamnolker, B. Nitzan, T. Tennenbaum, B. Bar-Toov, M. Hinz, H. Seliger, in *Scientific and Clinical Applications of Magnetic Carriers*, ed. U. Hafeli, Plenum Press, New York, 1997; (*b*) H. Baumnolker, B. Nitzan, S. Gura and S. Margel, *J. Mater. Sci. Lett.*, 1997, **16**, 1412; (*c*) S. Margel, I. Burdygin, V. Reznikov, B. Nitzan, O. Melamed, M. Sadeh, S. Gura, G. Mandel, M. Zuberi, L. Boguslavsky, in *Recent Research Developments in Polymer Science*, ed. S. G. Patidalai, Transworld Research Network, 1997, Vol. 1, 51–78; (*d*) S. Margel, I. Burdygin, S. Gura, H. Bamnolker, B. Nitzan, M. Kedem, O. Melamed, M. Zuberi, J. Mandel, L. Boguslavsky, L. Sheihet, T. Tennenbaum and B. Bar-Toov, *Nippon Oyo Jiki Gakkaishi*, 1998, **22**(S1), 429.
41 J. E. Baldwin, C. D. Jesudason, M. G. Moloney, D. R. Morgan and A. J. Pratt, *Tetrahedron*, 1991, **47**, 5603–5614.
42 L. Horner and E. H. Winkelmann, *Angew. Chem.*, 1959, **71**, 349–392.
43 (*a*) G. Li and R. Bittman, *Tetrahedron Lett.*, 2000, 6737–6741; (*b*) C. W. G. Fishwick and J. M. Sanderson, *Tetrahedron Lett.*, 1994, 4611–4614; (*c*) A. P. Marchand and K. A. Kumar, *Tetrahedron*, 1998, 15105–15112; (*d*) W. R. White, M. G. Platz, N. Chen and M. Jones, *J. Am. Chem. Soc.*, 1990, 7794–7796; (*e*) J. E. Baldwin, C. D. Jesudason, M. G. Moloney, D. R. Morgan and A. J. Pratt, *Tetrahedron*, 1991, 5603–5614.
44 K. A. Jacobson, B. Fischer and X. Ji, *Bioconjugate Chem.*, 1995, **6**, 255–263.
45 B. Fischer, J. L. Boyer, C. H. V. Hoyle, A. V. Ziganshin, A. L. Brizzolara, G. E. Knight, J. Zimmet, G. Burnstock, T. K. Harden and K. A. Jacobson, *J. Med. Chem.*, 1993, **36**, 3937–3946.
46 M. R. Maurizi and A. Ginsburg, *Biochemistry*, 1986, **25**, 131–140.
47 S. V. Kulikov and M. A. Samartsev, *Khim. Prir. Soedin.*, 1987, **4**, 613–614.
48 F. Wolfgang and C. Friedrich, *Nucleic Acid Chem.*, 1964, **143**, 827–836.
49 R. E. Humphrey, M. H. Ward and W. Hinze, *Anal. Chem.*, 1970, **42**, 698.
50 H. Bergmeyer, H. Grassl, H-E. Walter and H. U. Bergmeyer, eds. *Methods of Enzymatic Analysis*, 3rd ed., 1983, vol. 2, p. 222.
51 (*a*) A. Traverso-Cori, H. Chaimovich and O. Cori, *Arch. Biochem. Biophys.*, 1965, **109**, 173–184; (*b*) personal observation.
52 A. A. Baykov, O. A. Evtushenko and S. M. Avaeva, *Anal. Biochem.*, 1988, **171**, 266–270.
53 T. P. Geladopoulos, T. G. Sotiroudis and A. E. Evangelopoulos, *Anal. Biochem.*, 1991, **192**, 112–116.
54 M. Zofall and B. Bartholomew, *Nucleic Acids Res.*, 2000, **28**, 4382–4390.
55 A. N. Mayer and F. Barany, *Gene*, 1995, **153**, 1–8.
56 H. Bamnolker and S. J. Margel, *J. Polym.Sci., Chem. Ed.*, 1996, **34**, 1857–1871.
57 W. Stober, A. Fink and E. Bohn, *J. Colloid Interface Sci.*, 1968, **26**, 62–69.
58 P. Wikstrom, C. F. Mandenius and P. O. Larsson, *J. Chromatogr.*, 1988, **455**, 105–117.
59 J. Sevigny, F. P. Levesque, G. Grondin and A. R. Beaudoin, *Biochim. Biophys. Acta*, 1997, **1334**, 73–88.
60 M. M. Bradford, *Anal. Biochem.*, 1976, **72**, 248–254.
61 A. M. Kettlun, L. Uribe, V. Calvo, S. Silva, J. Rivera, M. Mancilla, M. A. Valenzuela and A. Traverso-Cori, *Phytochemistry*, 1982, **21**, 551–558.